J. Fluid Mech. (2015), *vol.* 781, *pp.* 578–594. © Cambridge University Press 2015
doi:10.1017/jfm.2015.508

Slip-induced suppression of Marangoni film thickening in surfactant-retarded Landau–Levich–Bretherton flows

David Halpern[1], Yen-Ching Li[2] and Hsien-Hung Wei[2,†]

[1]Department of Mathematics, University of Alabama, Tuscaloosa, AL 35487, USA

[2]Department of Chemical Engineering, National Cheng Kung University, Tainan 701, Taiwan

(Received 9 July 2014; revised 7 August 2015; accepted 25 August 2015;
first published online 24 September 2015)

We report that the well-known Marangoni film thickening in surfactant-laden Landau–Levich–Bretherton coating flow can be completely suppressed by wall slip. The analysis is made by mainly looking at how the deposited film thickness varies with the capillary number Ca ($\ll 1$) and the dimensionless slip length $\Lambda = \lambda/R$ ($\ll 1$) in the presence of a trace amount of insoluble surfactant, where λ is the slip length and R is the radius of the meniscus. When slip effects are weak at sufficiently large Ca (but still $\ll 1$) such that $Ca \gg \Lambda^{3/2}$, the film thickness can still vary as $Ca^{2/3}$ and be thickened by surfactant as if wall slip were absent. However, when slip effects become strong by lowering Ca to $Ca \ll \Lambda^{3/2}$, the film, especially when surface diffusion of surfactant is negligible, does not get thinner according to the strong-slip quadratic law reported previously (Liao *et al.*, *Phys. Rev. Lett.*, vol. 111, 2013, 136001; Li *et al.*, *J. Fluid Mech.*, vol. 741, 2014, pp. 200–227). Instead, the film behaves as if both surfactant and wall slip were absent, precisely following the no-slip 2/3 law without surfactant. Effects of surface diffusion are also examined, revealing three distinct regimes as Ca is varied from small to large values: the strong-slip quadratic scaling without surfactant, the no-slip 2/3 scaling without surfactant and the film thickening along the no-slip 2/3 scaling with surfactant. An experiment is also suggested to test the above findings.

Key words: interfacial flows (free surface), lubrication theory, thin films

1. Introduction

The goal of a coating process is to deposit a thin fluid layer with a desired thickness over a solid surface. This can be simply achieved hydrodynamically by pulling a plate (or a fibre) out of a bath of liquid (Landau & Levich 1942). If the coating is on the inside of a tube, film deposition can be realized by displacing the sample fluid using a long air bubble (Bretherton 1961). In either case, the film thickness can be precisely controlled by the coating speed U through a balance between viscous and surface tension forces. This so-called Landau–Levich–Bretherton (LLB) problem not only possesses common features of many coating flows seen in practice (Wilson

† Email address for correspondence: hhwei@mail.ncku.edu.tw

1982; Campanella & Cerro 1984; Quéré 1999), but also is closely relevant to dynamic wetting and drop spreading (de Gennes 1985; Kalliadasis & Chang 1994; Stone 2010; Liao, Li & Wei 2013; Li *et al.* 2014). Hence, it is of fundamental importance to many problems in interfacial fluid mechanics.

It is well known that for this kind of problem the deposited film thickness varies as $Ca^{2/3}$, where Ca is the capillary number (Landau & Levich 1942; Bretherton 1961), measuring the relative importance between viscous forces and surface tension forces. This result was originally derived for clean-interface systems without surfactant. While the 2/3 law has been confirmed experimentally, the measured film thickness appears to be slightly thicker than the clean-interface result (Bretherton 1961). This film thickening is commonly attributed to interfacial contamination by impurities or surface-active agents such as surfactants. Several theoretical and experimental investigations (Ratulowski & Chang 1990; Park 1991; Ramdane & Quéré 1997; Shen *et al.* 2002) with surfactants support this view. Specifically, surfactant sweeping by capillary draining towards the meniscus tends to lower the interfacial surfactant concentration at the film end. This non-uniform surfactant distribution in turn establishes a surface tension gradient opposing capillary draining, thereby generating a Marangoni shearing to thicken the film. For an insoluble surfactant, this film can be thickened at most by a factor of $4^{2/3}$ due to immobilization of the interface (Park 1991). The same thickening factor was actually first reported by Ratulowski & Chang (1990) in their study with soluble surfactant. More recent developments on how surfactant influences the film thickness can be seen in the works of Krechetnikov & Homsy (2006) and Delacotte *et al.* (2012).

The widely accepted results mentioned above are based on the usual no-slip condition applied at the walls. However, this condition does not always hold. For instance, in situations involving polymeric fluids (de Gennes 1985) and hydrophobic/textured surfaces (Choi & Kim 2006), apparent wall slip often exists. One might think that wall slip merely reduces drag and does not change no-slip flow characteristics. Recent studies on the Bretherton problem without surfactant show that the usual 2/3 law can change to a quadratic law when slip effects become strong for Ca below some critical value (Liao *et al.* 2013; Li *et al.* 2014). In another related study on the thermocapillary motion of a long bubble in a slippery tube, the dependence of the bubble speed on the applied temperature gradient over the bubble can change from the no-slip 5/3 law to the strong-slip cubic law (Liao *et al.* 2014). All of these studies indicate that wall slip can cause not only quantitative but also qualitative changes in flow characteristics, occurring when the film thickness b becomes much smaller than the slip length λ. That is, a flow characteristic change arises when the transverse length scale switches from b for the no-slip regime ($b \gg \lambda$) to λ for the strong-slip regime ($b \ll \lambda$). In fact, such a no-slip-to-slip transition is not limited to the LLB problem, but also occurs in dynamic wetting as well as interfacial instability (Liao *et al.* 2013). Hence, this transition should be a generic feature for a wide range of interfacial flows when wall slip is present.

In this paper we extend the length-scale-change idea mentioned above to the surfactant-laden LLB problem by examining how wall slip influences the Marangoni film thickening phenomenon. Whether film thickening can still persist in the presence of wall slip is not obvious. This is because, while wall slip can promote film thickening by facilitating Marangoni pumping into the film, it can equally make the film thinner by speeding up capillary draining out of the film (Li *et al.* 2014). Much to our surprise, it turns out that film thickening can be completely suppressed by wall slip at sufficiently low Ca where slip effects are strong. More precisely, even though

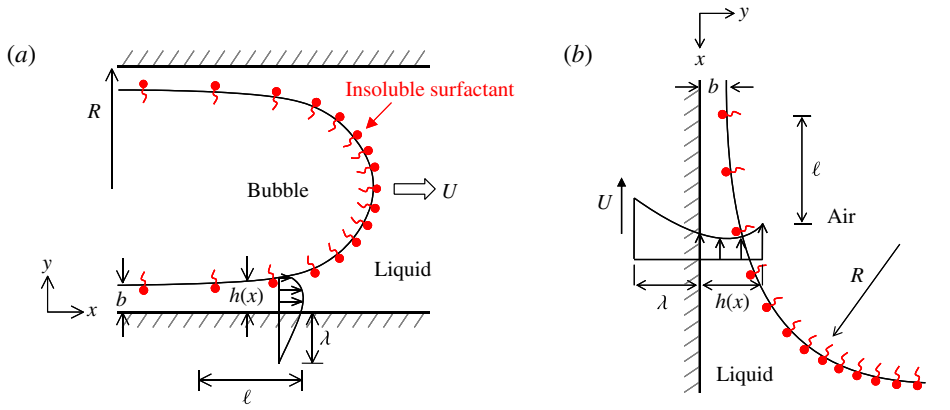

FIGURE 1. (Colour online) Flow geometries for the Landau–Levich–Bretherton problem with wall slip in the presence of insoluble surfactant. (*a*) The Bretherton problem for a bubble moving with a constant velocity in a slippery tube, which is the focus of the present work. (*b*) The Landau–Levich coating problem by pulling a slippery plate out of a bath of a liquid. Here, we focus on the transition film region of length $\ell \sim (bR)^{1/2}$ between the uniform film region of thickness b and the round meniscus region. $h(x)$ is the local film thickness in the transition region. The transition length $\ell \sim (bR)^{1/2}$ comes from the balance of the Laplace pressures between that of the film, $\sigma_0 b/\ell^2$, and that of the meniscus, σ_0/R. In (*b*), R is taken as the capillary length $(\sigma_0/\rho g)^{1/2}$, where ρ is the density of the liquid and g is gravitational acceleration.

the interface can be completely immobilized by surfactant (when surface diffusion is negligible), wall slip in effect can remobilize the entire film flow, making the film behave like one without surfactant in thickness, exactly described by the usual 2/3 law without any thickening.

This paper is organized as follows. In § 2, we begin with the lubrication theory to describe how the film changes its thickness due to both wall slip and surfactant effects. Numerical results and discussion are presented in § 3. In § 4, we make connections to experiments and propose ways to test our findings. Conclusions are given in § 5.

2. Lubrication theory

In this paper we focus our attention on the axisymmetric Bretherton problem with a trace amount of insoluble surfactant in a cylindrical tube of radius R (see figure 1*a*). Here, the tube wall is slippery, characterized by the slip length λ. Our analysis is equally applicable to Landau–Levich dip coating over a slippery plate, with the meniscus radius R being the capillary length (see figure 1*b*). The present approach largely follows Park (1991). The only difference here is that the no-slip condition is replaced by the Navier slip condition. As will be seen shortly, this additional slip term will have a significant impact on the deposited film thickness, and its combined effect with surfactant will lead to results that are completely different from those reported previously.

To begin with, we need a model to describe how the surface tension σ decreases with the surface concentration Γ. Let σ_0 be the surface tension at the static state with the corresponding surface concentration Γ_0. If the surfactant layer can be crudely treated as a 2D ideal gas, the linear equation of state $\sigma = \sigma_{clean} - k_B T\Gamma$ can be

assumed (Ramdane & Quéré 1997), where σ_{clean} is the surface tension of a clean interface without surfactant and k_BT is the thermal energy. Therefore, in the reference to the static state, we can rewrite the equation of state as $\sigma = \sigma_0(1 - M\gamma)$. Here, $M \equiv -(\Gamma_0/\sigma_0)(\partial\sigma/\partial\Gamma)_{\Gamma_0} = (\sigma_{clean} - \sigma_0)/\sigma_0$ is the Marangoni number (kept $O(1)$), which reflects the ability to lower surface tension (because of the minus sign here), and $\gamma \equiv \Gamma/\Gamma_0 - 1$ measures the extent of the surface excess concentration relative to Γ_0.

It is well known that there is an abrupt change in curvature and hence pressure in a small transition region between the bubble cap region and the uniform film region of thickness b. We employ lubrication theory to analyse the flow field and the bubble shape in the transition film region of length $\ell \sim (bR)^{1/2}$ (which comes from the balance of the Laplace pressures between that of the film, $\sigma_0 b/\ell^2$, and that of the meniscus, σ_0/R). Let $\hat{x} = x/R$ and $\hat{y} = y/R$ be the dimensionless spatial variables in the horizontal and transverse directions respectively. To better see the relative importance between relevant effects in the transition film region, it is convenient to rescale the horizontal and transverse length scales as $X = \hat{x}/Ca^{1/3}$ and $Y = \hat{y}/Ca^{2/3}$ using Bretherton's scalings (Park 1991), where $Ca = \mu U/\sigma_0$ is the capillary number which is assumed to be small ($\ll 1$). We define the dimensionless film thickness as $H(X) = h/(RCa^{2/3})$ using the same vertical length scale used to non-dimensionalize the vertical coordinate y given above. Let $\tilde{u} = u/U$ be the dimensionless velocity in the horizontal direction. The dimensionless transverse velocity is then $\tilde{v} = v/(UCa^{1/3})$ because of the continuity equation. With these rescaled variables, we can rescale the surface excess concentration as $G = \gamma/Ca^{2/3}$ by allowing the Marangoni stress $M\gamma_{\hat{x}} = (M/Ca^{1/3})\gamma_X$ to be comparable to the viscous stress $Ca\,\tilde{u}_{\hat{y}} = Ca^{1/3}\tilde{u}_Y$ in the tangential stress condition (Ratulowski & Chang 1990; Park 1991; Ramdane & Quéré 1997). Moreover, let $\tilde{p} = p/(\sigma_0/R)$ be the dimensionless pressure normalized by the Laplace pressure σ_0/R. In the frame moving with the bubble, the leading-order governing equations and boundary conditions (for which we drop the tildes for simplicity) are as follows:

$$u_X + v_Y = 0, \tag{2.1}$$

$$p_X = u_{YY}, \tag{2.2}$$

$$p = -H_{XX} \quad \text{at } Y = H, \tag{2.3}$$

$$u_Y = -MG_X \quad \text{at } Y = H, \tag{2.4}$$

$$u + 1 = \overline{\Lambda} u_Y \quad \text{at } Y = 0, \tag{2.5}$$

$$[u(1 + Ca^{2/3}G)]_X = \overline{D}G_{XX} \quad \text{at } Y = H. \tag{2.6}$$

Here, (2.1) and (2.2) are the continuity equation and the equation of motion in the horizontal direction respectively, and (2.3) is the Laplace pressure responsible for capillary draining (Bretherton 1961). It should be noted that because of the cylindrical interface, there should be an additional contribution from the circumferential curvature in (2.3). However, this term is $O(Ca^{2/3})$ and is hence negligible here. Equation (2.4) is the tangential stress condition accounting for the Marangoni shearing (Park 1991), (2.5) is the Navier slip condition (in the moving frame, Matthews & Hill 2009) with $\overline{\Lambda} = \Lambda/Ca^{2/3}$ and $\Lambda = \lambda/R$, and (2.6) is the surfactant transport equation along the interface of the film (Park 1991) with $\overline{D} = D/Ca^{2/3}$ and D the inverse of the surface Péclet number based on the capillary velocity σ_0/μ.

In (2.5), while $\Lambda = \lambda/R$ measures the amount of wall slip with respect to the tube radius R, the actual extent of wall slip in the film is reflected by the dynamic

slip parameter $\overline{\Lambda} = \Lambda/Ca^{2/3} = \lambda/b_0$ with respect to the Bretherton film thickness $b_0 \sim RCa^{2/3}$ for the no-slip case without surfactant. This parameter can be understood by looking at how the extent of wall slip is increased by decreasing the film thickness by lowering Ca (Li *et al.* 2014). At sufficiently large Ca (but still $\ll 1$), the film can be made sufficiently thick compared with the slip length λ. In this case, the film would behave like one without slip according to the Bretherton 2/3 law $b_0 \sim RCa^{2/3}$. Hence, this weak-slip situation corresponds to $\lambda/b_0 \ll 1$ or $\overline{\Lambda} \ll 1$. However, on lowering Ca along the 2/3 law to the point where the film thickness is comparable to λ, i.e. $\lambda/b_0 \sim 1$ or $\overline{\Lambda} \sim 1$, slip effects start to become important. Further lowering Ca makes the film thinner than λ, which corresponds to the strong-slip regime, signified by $\lambda/b_0 \gg 1$ or $\overline{\Lambda} \gg 1$. Therefore, on decreasing Ca from large to small values, one would experience a no-slip-to-slip transition from the weak-slip regime to the strong-slip regime. We emphasize that to solve for the problem, it is necessary to specify $\Lambda = \lambda/R$ for the amount of wall slip so that one can use $\overline{\Lambda}$ to evaluate whether slip effects are important in the film, depending on Ca. Even though Λ is typically small, slip effects could be strong since the film thickness can be made comparable to or smaller than the slip length. As will be demonstrated later in § 3, even though the amount of wall slip (with respect to R) is 1 % (i.e. $\Lambda = 0.01$), it is still enough to completely suppress Marangoni film thickening.

It is worth mentioning how the surfactant transport equation (2.6) is derived. An inspection of the full surfactant transport equation in dimensional form (Stone 1990) reveals that the term due to the interface expansion/contraction, $\Gamma v/R \sim Ca^{1/3}U\Gamma_0/R$, is much smaller than the term due to surface convection along the interface, $(\Gamma u)_x \sim (U\Gamma_0/R)Ca^{-1/3}$. Hence, the surfactant transport equation here can be taken as an approximate form by keeping the surface convection term $[u(1+\gamma)]_X = [u(1+Ca^{2/3}G)]_X$ as the primary contribution in the surfactant transport along the film (Park 1991). To emphasize $O(Ca^{2/3})$ surfactant concentration variations under $Ca \ll 1$, we keep $Ca^{2/3}G$ in (2.6) at this moment. This term will be neglected later. We also take into account surface diffusion of surfactant and use $\overline{D} = D/Ca^{2/3}$ to reflect its importance relative to surface convection (Park 1991), where $D \equiv 1/Pe_s$ is the inverse of the surface Péclet number $Pe_s = \sigma_0 R/\mu D_s$, which is based on the capillary velocity σ_0/μ and the surface diffusion coefficient of surfactant D_s. Since the flow here is steady in the frame of the bubble, there is no time derivative term in (2.6).

Ignoring the $O(Ca^{2/3})$ term, we integrate (2.6) once and apply the downstream condition $u \to -1$ as $X \to -\infty$. This reduces (2.6) to

$$u = \overline{D}G_X - 1 \quad \text{at } Y = H, \tag{2.7}$$

which simply states that the net surface convective flux $u(Y = H) + 1$ is exactly counterbalanced by the surface diffusion flux $-\overline{D}G_X$ (Park 1991). In the special case where surface diffusion is negligible ($\overline{D} = 0$), (2.7) leads to $u(Y = H) = -1$ everywhere along the interface, meaning that the interface is completely immobilized by surfactant.

With (2.1)–(2.5) and (2.7), the relevant differential equation for H can be readily derived below. We first determine the horizontal velocity by integrating (2.2) subject to (2.4) and (2.5). This leads to

$$u = \frac{p_X}{2}[Y^2 - 2H(Y + \overline{\Lambda})] - MG_X(Y + \overline{\Lambda}) - 1, \tag{2.8}$$

where G_X is expressed in terms of p_X by applying (2.7),

$$G_X = -\frac{1}{2}p_X\left[\frac{H^2+2H\overline{\Lambda}}{M(H+\overline{\Lambda})+\overline{D}}\right]. \tag{2.9}$$

Next, we equate the volumetric flux (per unit width) in the transition film region to that in the uniform film region of (unknown) thickness $B \equiv b/(RCa^{2/3})$, which is the direct consequence of (2.1). This yields

$$\int_0^H u\,\mathrm{d}Y = -B. \tag{2.10}$$

Obtaining the flow rate by integrating the velocity profile (2.8) across the film, (2.10) leads to

$$-\frac{p_X}{3}(H^3+3H^2\overline{\Lambda}) - \frac{MG_X}{2}(H^2+2\overline{\Lambda}H) = H - B. \tag{2.11}$$

Eliminating G_X using (2.9) and making use of (2.3), we can rewrite (2.11) as the following differential equation for H:

$$SH^3H_{XXX} = 3(H-B), \tag{2.12a}$$

where $S = S(H)$ and is defined as

$$S \equiv 1 + 3\frac{\overline{\Lambda}}{H} - \frac{3}{4}\frac{MH(1+2\overline{\Lambda}/H)^2}{MH(1+\overline{\Lambda}/H)+\overline{D}}. \tag{2.12b}$$

The factor S measures how the strength of the apparent capillary flow (relative to pure capillary draining of the no-slip clean-interface case) varies with wall slip and surfactant effects. Because this flow tends to thin the film, the larger S becomes the thinner the film. As will be seen later in the discussion after (2.15), S will determine whether the film gets thinner or thicker due to the combined effects of wall slip and surfactant, and hence the film thickening factor b/b_0, where b/b_0 is taken to be the film thickness ratio with respect to the no-slip clean-interface one, $b_0 \equiv b$ $(M=0,\ \Lambda=0)$ with $S=1$. Rescaling (H, B, X) as $(H/S^{2/3}, B/S^{2/3}, X/S^{1/3})$, (2.12*a*) can be transformed back to the classical Bretherton equation with no slip and no surfactant. The rescaling $B/S^{2/3}$ also means that the film thickening factor $b/b_0 = 1/S^{2/3}$. We emphasize that while the transformation above suggests that (2.12*a*) is mathematically equivalent to the classical Bretherton equation, new physics is actually brought out by S. The transformation is meant to illuminate the role of S in controlling the film thickness by comparing (2.12*a*) with the classical Bretherton equation.

To solve (2.12), the following boundary conditions have to be imposed by requiring the interface profile to match those at the uniform thin-film end and the round meniscus end (Park 1991):

$$H \to B, \quad H_X \to 0, \quad H_{XX} \to 0 \quad \text{as } X \to -\infty, \tag{2.13a–c}$$

$$H_{XX} \to 1 \quad \text{as } X \to \infty. \tag{2.14}$$

Here, (2.14) comes from matching the Laplace pressure $\sigma_0 h_{xx}$ in the transition film region to the bubble cap σ_0/R. After solving for H, the excess surface concentration G can then be readily found by solving (2.9) with $G(X \to -\infty) = G_0$ (constant) (Park 1991).

Equation (2.12) is the central equation of this paper and describes how the film thickness behaves under the combined influence of surfactant and wall slip effects. The equation is translational invariant because it will not change at all if one shifts the origin of X. This is easily understood because the interface shape (and hence the film thickness B) will not depend on where the origin is defined. We should also remark that the equation only holds for $M \neq 0$, which renders the Marangoni stress $-MG_X$ in (2.4), and is also the prerequisite of the surface diffusion term $\overline{D}G_{XX}$ in (2.6). (That is, $\overline{D}$ has to be set to be zero when $M = 0$; otherwise $S(M = 0, \overline{\Lambda} = 0)$ will not be equal to 1, contradicting the requirement $S = 1$ for the no-surfactant and no-slip case.) Whether the film gets thinner or thicker is controlled by S given by (2.12*b*). The factor S can be raised by wall slip (via $3\overline{\Lambda}/H$) which promotes capillary draining out of the film, which tends to thin the film. On the other hand, S can be decreased by the Marangoni shearing towards the film due to surfactant (via the negative M term), which tends to thicken the film. However, this film thickening effect cannot be increased indefinitely by increasing M, since the surface concentration gradient (and hence the Marangoni stress) will be diminished by surface convection (via the denominator of (2.9)). Similarly, such film thickening can also be mediated by wall slip in that while the Marangoni pumping is compensated by surface convection with a factor $(1 + \overline{\Lambda}/H)$, it can be enhanced by wall slip with a factor $(1 + 2\overline{\Lambda}/H)^2$.

In the special case where surface diffusion is negligible ($\overline{D} = 0$), (2.12*b*) is equal to

$$S = \frac{1}{4}\left(\frac{1 + 4\dfrac{\overline{\Lambda}}{H}}{1 + \dfrac{\overline{\Lambda}}{H}}\right), \tag{2.15}$$

which is independent of $M\,(\neq 0)$. Hence, for an arbitrary non-zero M (but kept $O(1)$), in the weak-slip regime, $\overline{\Lambda} \ll 1$ or $Ca \gg \Lambda^{3/2}$ yields $S = 1/4$, reducing (2.12*a*) to

$$H^3 H_{XXX} = 12(H - B). \tag{2.16}$$

This is essentially the Bretherton equation, but on the right-hand side of (2.16), the usual factor of 3 for the clean-interface case is replaced by 12, giving the well-known maximum film thickening factor of $4^{2/3}$ (Ratulowski & Chang 1990; Park 1991) as a result of complete immobilization of the air–liquid interface by surfactant. The $4^{2/3}$ factor here comes from the fact that (2.16) can be transformed from the no-slip Bretherton equation without surfactant (2.17) (see below) by rescaling (H, B, X) as $(4^{2/3}H, 4^{2/3}B, 4^{1/3}X)$. It should be noted that if one assumes the interface to be no-slip everywhere, i.e. $u(Y = H) = -1$, and solves the problem without using the tangential condition (2.4), one would end up with $H^3 H_{XXX} = 6(H - B)$, which leads the thickening factor to be $2^{2/3}$ (Bretherton 1961; Schwartz, Princen & Kiss 1986) (again, this $2^{2/3}$ factor can be realized by transforming the coefficient '3' into '6' in (2.17) after rescaling (H, B, X) as $(2^{2/3}H, 2^{2/3}B, 2^{1/3}X)$ in (2.17)).

Conversely, in the strong-slip regime where $\overline{\Lambda} \gg 1$ or $Ca \ll \Lambda^{3/2}$ with surfactant, we have $S = 1$ in (2.15), reducing (2.12*a*) to the no-slip Bretherton equation without surfactant exactly,

$$H^3 H_{XXX} = 3(H - B). \tag{2.17}$$

As a result, the film thickness will exactly follow Bretherton's 2/3 law $b/R \sim Ca^{2/3}$. This is a very surprising result since wall slip and surfactant effects together make the film behave as if both were absent!

Why (2.17) is very surprising can also be seen by comparing it with the strong-slip case without surfactant. The equation for the latter case can be obtained by first eliminating the M term in (2.12) and then taking $\overline{\Lambda} \gg 1$ (Liao *et al.* 2013; Li *et al.* 2014), yielding

$$\overline{\Lambda} H^2 H_{XXX} = H - B. \tag{2.18a}$$

The scaling of the film thickness for this case can be obtained by balancing the terms in (2.18*a*) using $H \sim B$ (because $h \sim b$) and $X \sim B^{1/2}$ (because $\ell \sim (bR)^{1/2}$), giving $B \sim \overline{\Lambda}^{-2}$ or

$$b/R \sim Ca^2 R^2/\lambda^2. \tag{2.18b}$$

This is much thinner than the no-slip result $b/R \sim Ca^{2/3}$ without surfactant because capillary draining out of the film, which tends to thin the film, becomes much more intensified by wall slip (Liao *et al.* 2013; Li *et al.* 2014). As the strong-slip case with surfactant (2.17) also leads to a much thicker film $b/R \sim Ca^{2/3}$ than (2.18*b*) without surfactant, this implies that the Marangoni shearing towards the film is also enhanced by wall slip. This slip-enhanced shearing is so strong that it is able to completely compensate the equally intensified capillary draining, which in turn thickens the film back to the no-slip result without surfactant.

Alternatively, although the interface is immobilized by surfactant (see (2.7) with $\overline{D} = 0$), wall slip in effect can remobilize the entire film flow. More importantly, the film does not get thinner by wall slip by lowering Ca, contrary to the strong-slip case (2.18) without surfactant. Instead, it behaves just like the clean-interface case (2.17) without slip. Therefore, compared with the no-slip case with surfactant, the Marangoni film thickening is completely suppressed by wall slip. Indeed, on inspecting the velocity profile (2.8) for this strong-slip scenario, we find that the slip part of the Marangoni flow, $-MG_X\overline{\Lambda} \approx p_X H\overline{\Lambda}$ (because of (2.9)), is exactly cancelled out by the slip part of the capillary flow, $-p_X H\overline{\Lambda}$. This reduces (2.8) to

$$u = \frac{p_X}{2}(Y^2 - H^2) - 1. \tag{2.19}$$

As a result, even though the air–liquid interface is immobilized by surfactant (see (2.7) with $\overline{D} = 0$), the film flows in a purely capillary manner, independent of M ($\neq 0$). More precisely, it flows in such a way that the velocity minimum (in magnitude) is shifted onto the slippery wall. The reason for this result is that the velocity increment by wall slip is mainly manifested by the $\overline{\Lambda}$ terms in (2.8). While wall slip can prompt the Marangoni shearing towards the film via $-MG_X\overline{\Lambda}$, it can equally speed up capillary draining out of the film via $-p_X H\overline{\Lambda}$. When slip effects are strong, these two linear flows completely cancel each other out, leaving the Laplace pressure gradient (i.e. the Y^2 term in (2.8) and the H^2 term in (2.9)) alone to drive the film. This explains (2.19) and hence the complete suppression of the film thickening by wall slip.

Combining both (2.16) for $\overline{\Lambda} \ll 1$ and (2.17) for $\overline{\Lambda} \gg 1$ discussed above for the case with negligible surface diffusion, we conclude that the film thickness always scales as $Ca^{2/3}$. Specifically, when $Ca \gg \Lambda^{3/2}$ the film can be thickened by surfactant in the no-slip manner according to (2.16). However, on lowering Ca to the regime where $Ca \ll \Lambda^{3/2}$, the film can be thinned back to the result without surfactant on a no-slip wall according to (2.17). The transition between film thickening (with respect to the no-slip case without surfactant) and film thinning (with respect to the slip case with

surfactant) occurs at $\overline{\Lambda} \sim 1$ or $Ca \sim Ca^* \equiv \Lambda^{3/2}$, just like the Bretherton problem in a slippery tube without surfactant (Liao *et al.* 2013; Li *et al.* 2014).

If surface diffusion is included, we anticipate that the effects will diminish surfactant concentration gradients, which will in turn reduce the Marangoni film thickening. It is obvious that $D \to \infty$ will completely suppress surfactant concentration gradients (see (2.9)), thereby making the film behave as the case without surfactant (i.e. the M term in (2.12) vanishes). In this case, wall slip tends to thin the film according to (2.18). Therefore, at a finite value of D, we anticipate that this slip-induced film thinning (without surfactant) can compete with the Marangoni film thickening (with surfactant). As will be shown later, how the film thickness is determined by this competition can be seen more clearly by looking at how the velocity profile changes by decreasing Ca from the no-slip ($Ca \gg \Lambda^{3/2}$) regime to the strong-slip ($Ca \ll \Lambda^{3/2}$) regime.

3. Results and discussion

To confirm the features discussed above, we integrate (2.12) numerically for the film with surfactant ($M \neq 0$) using a nonlinear shooting method. The equation is first linearized around $H = B$. One of the solutions, which grows exponentially towards the bubble cap region, is chosen as the profile near the uniform film end ($X = 0$), where H deviates from B with a very small amplitude. It is worth mentioning that (2.12), together with boundary conditions (2.13) and (2.14), is translational invariant. This provides convenience for constructing the linearized solution by choosing the origin $X = 0$ (Bretherton 1961). For a given B, we take values for H, H_X, and H_{XX} at $X = 0^+$ from the linearized solution and then integrate (2.12) towards the bubble cap region. The thickness of the uniform film region, B, is adjusted iteratively until (2.14) is satisfied. More details about the solution method can be seen in appendix A.

Figure 2(*a*) plots how b/R varies with Ca. In the absence of surfactant ($M = 0$), we recover the switch from the no-slip 2/3 law to the strong-slip quadratic law (Liao *et al.* 2013; Li *et al.* 2014). We also calculate the no-slip case with surfactant (at $M = 1$) by neglecting surface diffusion ($\overline{D} = 0$) in (2.12), confirming the $4^{2/3}$ (≈ 2.5) factor increase in b/R along the 2/3 law. As for the slip case, we again set $\overline{D} = 0$ and find that surfactant essentially causes the quadratic scaling to disappear. What may be really surprising is that even when the amount of wall slip is 1 % with respect to R ($\Lambda = 0.01$), it can completely suppress the Marangoni film thickening, thereby causing b/R to follow the 2/3 law in the entire $Ca \ll 1$ range. The thickening-to-thinning transition can be seen more clearly in figure 2(*b*) by plotting the thickening factor b/b_0 against Ca. It should be noticed that the results here are independent of M ($\neq 0$) because of (2.15).

The above results indicate that the situation combining both wall slip and surfactant behaves differently from the case when either effect exists alone. If surfactant is absent, wall slip tends to thin the film because of slip-intensified capillary draining out of the film (Liao *et al.* 2013; Li *et al.* 2014). This thinning can change the well-known 2/3 law to the quadratic law and is manifested most when slip effects become strong for $Ca < Ca^* = \Lambda^{3/2}$. When surfactant is present, however, we find that not only does the strong-slip quadratic law completely vanish, but also the entire curve essentially varies along the 2/3 law. Therefore, compared with the surfactant-free case, wall slip can also help film thickening. As the film without surfactant can now be thickened back to the 2/3 law with the aid of surfactant, this implies that the Marangoni shearing towards the film is also promoted by wall slip, which is again manifested in the strong-slip regime for $Ca < Ca^*$.

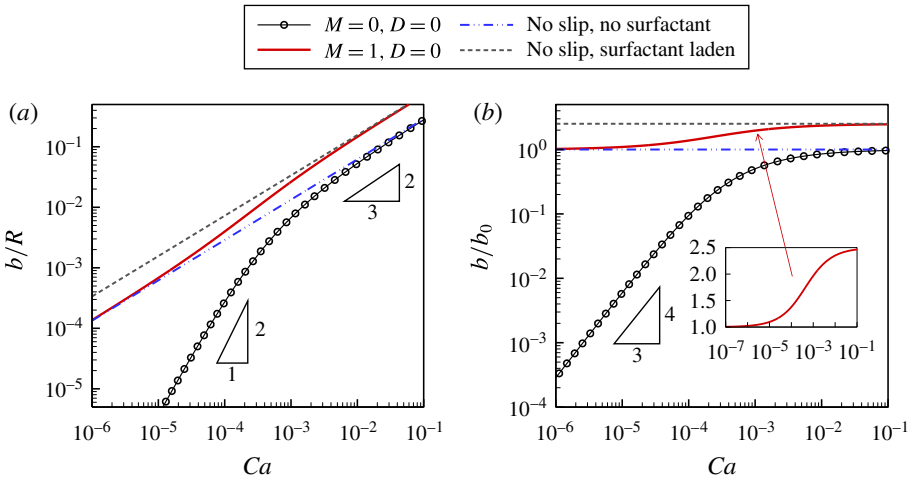

FIGURE 2. (Colour online) (*a*) Dependence of the dimensionless film thickness b/R on Ca at $\Lambda = 0.01$. In the absence of surfactant (the Marangoni number $M = 0$, solid line with circles), the well-known no-slip 2/3 law $b/R \sim Ca^{2/3}$ (blue dash-dotted line) can switch to the strong-slip quadratic law $b/R \sim Ca^2$ for Ca below a certain value. When surfactant is present and surface diffusion is negligible ($M = 1$ and $\overline{D} = 0$, red solid line), the film is thickened along the 2/3 law (dashed line) in the large-Ca (but still $\ll 1$) regime. However, for small Ca, the film does not get thinner according to the strong-slip quadratic law. Instead, it follows the no-slip 2/3 law without surfactant, indicating that the Marangoni film thickening can be completely suppressed by wall slip. (*b*) The corresponding thickening factor b/b_0 (with respect to the no-slip clean-interface result b_0) is plotted as a function of Ca. The result for the surfactant case (red solid line) shows that the maximum thickening factor $4^{2/3}$ (≈ 2.5) seen in the large-Ca regime can be reduced to 1 on decreasing Ca from large to small values, as can be seen more clearly in the inset. It should be noted that for $\overline{D} = 0$ the result is independent of M ($\neq 0$), as indicated by (2.15).

To see how the thickening-to-thinning transition is affected by wall slip, figure 3 plots the thickening factor b/b_0 against Ca for various values of Λ at $M = 1$ and $\overline{D} = 0$. It shows that the larger Λ is, the greater the Ca at which the transition takes place. This is obvious because the strong-slip $Ca \ll Ca^*$ regime extends to a larger $Ca^* = \Lambda^{3/2}$ as Λ is increased.

The above results, which exclude the influence of surface diffusion, basically confirm the features discussed in § 2. Inclusion of surface diffusion tends to lower surfactant concentration gradients. Therefore, one might anticipate that the result will return to the clean-interface one as $\overline{D} \to \infty$, as indicated by (2.12). However, for a given surface diffusion coefficient D_s, this erasing concentration gradient effect actually varies like $\overline{D} \propto Ca^{-2/3}$. Therefore, for any finite value of D_s, the Marangoni film thickening could still persist although it is gradually weakened by decreasing Ca. On the other hand, the slip term in (2.5) also varies like $\overline{\Lambda} \propto Ca^{-2/3}$ and is getting more important as Ca is decreased, which tends to thin the film in a manner like $b/R \sim Ca^2$ in the absence of surfactant (Liao *et al.* 2013; Li *et al.* 2014). Therefore, there is a competition between surfactant-induced film thickening and slip-induced film thinning.

Figure 4(*a*) shows surface diffusion effects on the film thickness by plotting the film thickening factor b/b_0 against Ca at $\Lambda = 0.01$ and $M = 1$ for various

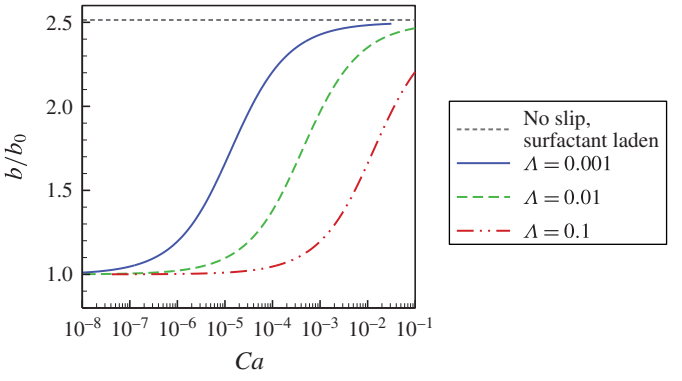

FIGURE 3. (Colour online) Plot of the film thickening factor b/b_0 against Ca for various values of Λ at $M = 1$ and $\overline{D} = 0$, showing that the thickening-to-thinning transition takes place at larger Ca as Λ is increased.

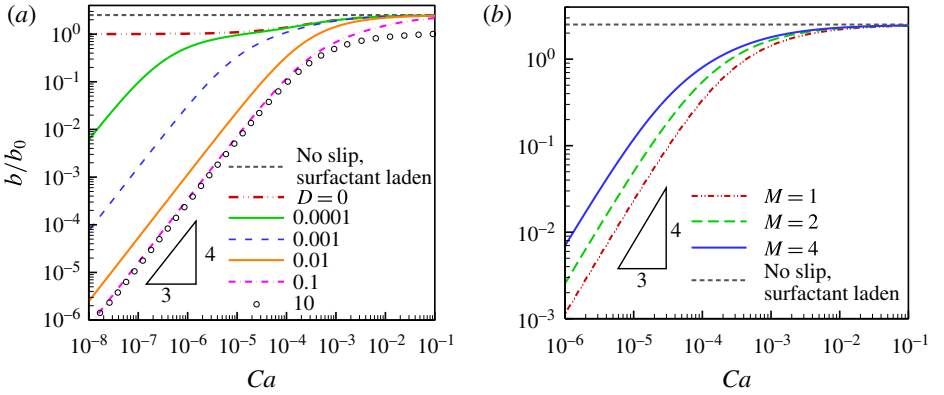

FIGURE 4. (Colour online) (*a*) Effects of surface diffusion on the film thickness by plotting the thickening factor b/b_0 against Ca for various values of $D \equiv 1/Pe_s$ indicated in the legend. Here, $\Lambda = 0.01$ and $M = 1$. For $D = 0.1$ or larger, the film thickness displays three distinct regimes as Ca is varied: the strong-slip quadratic scaling $b/R \sim Ca^2$ without surfactant (indicated by $b/b_0 \sim Ca^{4/3}$), the no-slip 2/3 scaling $b/R \sim Ca^{2/3}$ without surfactant (indicated by $b/b_0 \sim 1$) and the thickening along the no-slip 2/3 law with surfactant (indicated by $b/b_0 > 1$). (*b*) At given D and Λ, increasing M tends to thicken the film and thereby to shift the curve towards smaller Ca, as illustrated by plotting how b/b_0 varies with Ca for $M = 1$, 2 and 4 at $\Lambda = 0.01$ and $D = 0.01$.

values of $D \equiv 1/Pe_s$. Even for small D, the film thickness varies as $b/R \sim Ca^2$ or $b/b_0 \sim Ca^{4/3}$ when Ca is below a certain value, much like the strong-slip situation without surfactant (Liao *et al.* 2013; Li *et al.* 2014). It should be noticed that at a sufficiently large Ca the film still remains thicker than the no-slip case without surfactant. Increasing D makes the strong-slip scaling $b/R \propto Ca^2$ shift slightly towards a larger Ca. However, increasing D to 0.1 or higher does not make the strong-slip curve shift any further. This corresponds to the situation where the surfactant concentration gradient is completely erased by surface diffusion. Hence, for very small Ca, we recover the strong-slip result without surfactant (Liao *et al.* 2013; Li *et al.* 2014). However, since $\overline{D} = D/Ca^{2/3}$, surface diffusion effects become

weakened by convection as Ca is increased (see (2.7)). Together with the fact that the slip coefficient $\overline{\Lambda} = \Lambda/Ca^{2/3}$ is also diminished by increasing Ca, the film thickness follows the no-slip clean-interface result $b/R \sim Ca^{2/3}$ or $b/b_0 = 1$ when Ca is increased beyond a certain value. Yet, at a sufficiently large Ca, surface diffusion is completely suppressed by convection. This leads the surfactant concentration gradient to be re-established, thereby thickening the film again due to the restored Marangoni shearing. This is the reason why figure 4(*a*) shows the coexistence of the strong-slip result ($b/b_0 \sim Ca^{4/3}$) without surfactant, the no-slip clean-interface plateau ($b/b_0 = 1$) and the no-slip thicker film result ($b/b_0 > 1$) with surfactant. At given D and Λ, it is obvious that increasing M tends to thicken the film and hence to shift the curve towards smaller Ca, as shown in figure 4(*b*).

To better visualize how surface diffusion of surfactant influences the film thickening/thinning behaviour, figure 5 plots velocity profiles within the film for various values of Ca at $M = 1$, $D = 0.001$ and $\Lambda = 0.01$. Here, in conjunction with figure 4(*a*), the values of Ca are chosen to cover all possible regimes, from the no-slip regime ($Ca \gg Ca^*$) to the strong-slip regime ($Ca \ll Ca^*$), so that one can see more clearly how the Marangoni shearing gets enhanced or diminished so as to determine film thickening or thinning due to the combined effects of wall slip and surface diffusion, where $Ca^* = \Lambda^{3/2} = 10^{-3}$. Taking $Ca = 0.01$ ($\overline{\Lambda} \approx 0.22$, figure 5*a*) greater than Ca^*, the flow basically behaves like the no-slip case. Because $\overline{D} = D/Ca^{2/3} \approx 0.02$ here, surface diffusion is weak. Therefore, the film can be thickened by Marangoni shearing with the maximum thickening factor $4^{2/3}$. When Ca is decreased to 10^{-3} ($\overline{\Lambda} = 1.0$, figure 5*b*) or 10^{-4} ($\overline{\Lambda} \approx 4.64$, figure 5*c*), slip effects become more pronounced. In this case, compared with $Ca = 0.01$, the Marangoni shearing (towards the film) is enhanced, which tends to promote film thickening. However, capillary draining (out of the film), which tends to thin the film, is also equally enhanced by wall slip. Because the former is compensated by the latter, the resulting film thickening is slightly weaker than that at $Ca = 0.01$ (see figure 4*a*). However, when Ca is decreased to 10^{-5} ($\overline{\Lambda} \approx 21.54$, figure 5*d*) where slip effects become very strong, we find that the Marangoni shearing becomes weaker compared with that at $Ca = 10^{-4}$. This is because $\overline{D} = D/Ca^{2/3} \approx 2.15$ here, surface diffusion becomes effectively strong and hence greatly reduces surface concentration gradients. The situation here is like the strong-slip case without surfactant, explaining why the film becomes considerably thinner than those at larger Ca (see figure 4*a*).

4. Connections to experiments

In terms of experiments, we have not seen any studies that are specifically designed for testing how wall slip influences the film thickness b for the Bretherton/Landau–Levich problems with or without surfactant. Nevertheless, it is worth discussing the feasibility of such an experiment. First of all, apparent wall slip can be achieved by using polymeric liquids (e.g. silicone oil). For low molecular weights (having a degree of polymerization $>10^3$), the slip length λ can be as large as 1 μm (de Gennes 1985). Taking a capillary tube with a radius of $R \sim 100$ μm, the amount of wall slip is $\Lambda = \lambda/R \sim 0.01$. If the air–liquid interface is clean, Bretherton's 2/3 law $b/R \sim Ca^{2/3}$ still holds for Ca greater than the critical value $Ca^* \sim \Lambda^{3/2} \sim 10^{-3}$. However, for Ca below this value, the strong-slip quadratic scaling $b/R \sim Ca^2\Lambda^{-2}$ should be observed. In addition, to make the film thickness detectable but not too thick compared with the slip length (especially for confirming the strong-slip quadratic law), it would be better for the bubble to move at $U \sim 1$ cm s^{-1} (or $Ca \sim 10^{-3}$ for $\mu \sim 10^{-1}$ poise and

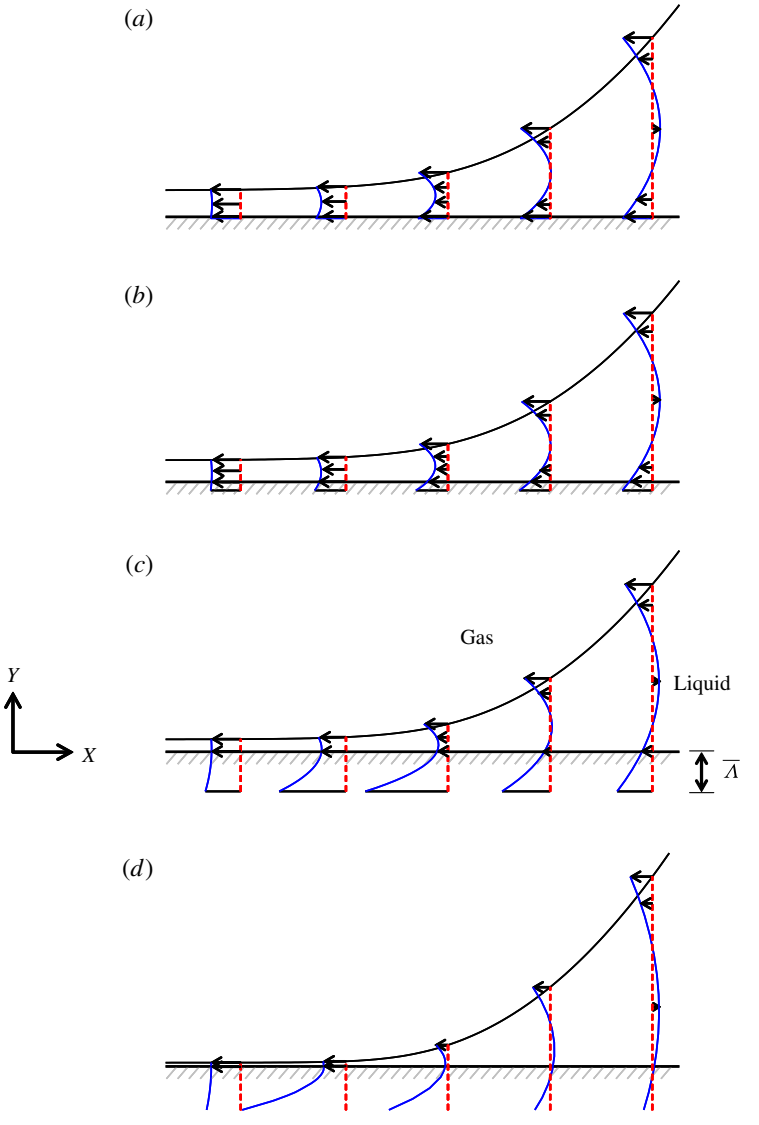

FIGURE 5. (Colour online) Calculated velocity and interface profiles for the Bretherton problem at $M = 1$, $\Lambda = 0.01$ and $D = 0.001$. Results are plotted in terms of rescaled variables $X = x/RCa^{1/3}$ and $Y = y/RCa^{2/3}$ in the frame moving with the bubble. As the interface profiles are represented by $H(X) = h/RCa^{2/3}$, the rescaled film thickness $H(X \to -\infty)$ can be roughly regarded as the film thickening factor. At (*a*) $Ca = 10^{-2}$, at which the effective slip coefficient $\overline{\Lambda} = \Lambda/Ca^{2/3} \approx 0.2$ is small, the situation behaves like the no-slip case. When Ca is decreased to (*b*) $Ca = 10^{-3}$ or (*c*) $Ca = 10^{-4}$, $\overline{\Lambda} = \Lambda/Ca^{2/3}$ ($\geqslant 1$) becomes significantly increased, although Marangoni shearing towards the film can be promoted by decreasing Ca, capillary draining out of the film is equally enhanced. Because the former is compensated by the latter, the resulting film thickening is slightly weaker than (*a*) at $Ca = 10^{-2}$. At (*d*) $Ca = 10^{-5}$, while slip effects are very strong with $\overline{\Lambda} \approx 21.54$, surface diffusion is also effectively strong with $\overline{D} = D/Ca^{2/3} \approx 2.15$. This greatly reduces surface concentration gradients, making the film thin as in the strong-slip situation without surfactant.

$\sigma_0 \sim 30$ dyn cm^{-1}) to ensure a film thickness in the range of 1–10 μm, like what is observed in the experiment using silicone oil (Piroird, Clanet & Quéré 2011).

For the case with surfactant, we take sodium dodecyl sulphate (SDS) in silicone oil (Piroird *et al.* 2011) as an example to illustrate the effects at work. For this system, $\sigma_{clean} \approx 35$ dyn cm^{-1} (the surface tension of silicone oil), $\mu \sim 10^{-1}$ poise (the viscosity of silicone oil) and $M = (\sigma_{clean} - \sigma_0)/\sigma_0$ ranges from 0.17 to 1.33 (where $\sigma_0 \approx 30$–15 dyn cm^{-1} for 1–10 % of the critical micelle concentration, see figure 2*b* of Piroird *et al.* 2011). The surface diffusion coefficient D_s has the same typical value as the diffusion coefficient in the bulk, $D_b \sim 10^{-7}$–10^{-6} cm^2 s^{-1} (in silicone oil) (Ramdane & Quéré 1997), giving the surface Péclet number $Pe_s = \sigma_0 R/\mu D_s$ to be of order 10^6–10^7. For a small capillary tube, it is likely that the time scale required for surfactant to absorb onto the interface is much longer than that for advecting surfactant over the transition length $\ell \sim (bR)^{1/2}$ (Ramdane & Quéré 1997). In this case, the surfactant acts as an insoluble surfactant, making the Marangoni film thickening most efficient (Ramdane & Quéré 1997). Moreover, because $Ca = \mu U/\sigma_0$ typically ranges from 10^{-5} to 10^{-2} for $U = 10$ μm s^{-1} to 1 cm s^{-1}, $\overline{D} = (Pe_s Ca^{2/3})^{-1}$ is of order 10^{-3} at most, and hence the surfactant transport is essentially dominated by surface convection. Thus, one might expect to observe film thickening and thinning along the 2/3 law without seeing the strong-slip quadratic law.

However, if one can select a surfactant such that its adsorption rate is sufficiently fast but not too fast (by, for instance, controlling the amount of surfactant) to completely erase the surfactant concentration gradient, the quadratic law might reappear along with the film thickening and thinning along the 2/3 law, just like figure 4.

Landau–Levich coating can be achieved by withdrawing a fibre or a plate out of a bath of a liquid. For fibre coating, the situation is pretty much the same as the Bretherton problem, except that R should be taken as the fibre radius. For plate coating, R is roughly the capillary length $(\sigma_0/\rho g)^{1/2} \sim 1$ mm, where $\rho \sim 1$ g cm^{-3} is the fluid density and g is the gravitational acceleration. In this case, in order to have discernible wall slip effects like $\Lambda = \lambda/R \sim 0.01$, λ would have to be as large as 10 μm, which can be achieved by using a high-molecular-weight polymeric liquid with a degree of polymerization $>10^3$.

5. Concluding remarks

We have demonstrated for the Bretherton problem with insoluble surfactant that the well-known Marangoni film thickening can be completely suppressed by wall slip effects, especially when surface diffusion is small or negligible. That is, in contrast to the clean-interface problem with wall slip, which shows that Bretherton's 2/3 law can turn to the strong-slip quadratic law for Ca below some critical value (Liao *et al.* 2013; Li *et al.* 2014), the film thickness here can still be described by the 2/3 law without undergoing further thinning by wall slip. In other words, while both Marangoni shearing towards the film and capillary draining out of the film can be enhanced by wall slip, the former can be compensated by the latter, which alleviates the Marangoni film thickening. We also find that surface diffusion can cause a competition between surfactant-induced film thickening and slip-induced film thinning. Because of this competition, how the film thickness varies with Ca can exhibit three distinct regimes as Ca changes from small to large values: the strong-slip quadratic scaling $b/R \sim Ca^2$ without surfactant, the no-slip 2/3 scaling $b/R \sim Ca^{2/3}$ without surfactant and the film thickening along the 2/3 law with surfactant. These different scaling results are summarized in table 1.

	No surfactant, $M=0$		With surfactant, $M\neq 0$	
	Weak slip, $\overline{\Lambda}\ll 1$	Strong slip, $\overline{\Lambda}\gg 1$	Weak slip, $\overline{\Lambda}\ll 1$	Strong slip, $\overline{\Lambda}\gg 1$
b/R	$Ca^{2/3}$	$Ca^{2}\Lambda^{-2}$	$Ca^{2/3}$	$Ca^{2/3}$ for $D=0$ $Ca^{2}\Lambda^{-2}$ as $D\to\infty$
b/b_0	1	$Ca^{4/3}\Lambda^{-2}$	$4^{2/3}$ for $D=0$ 1 as $D\to\infty$	1 for $D=0$ $Ca^{4/3}\Lambda^{-2}$ as $D\to\infty$

TABLE 1. Summary of various scaling results for the film thickness b/R and the film thickening factor b/b_0 (with respect to the no-slip result b_0 without surfactant). Here, $\overline{\Lambda}=\Lambda/Ca^{2/3}$ is the slip coefficient measuring the extent of wall slip in the film, with $\Lambda=\lambda/R$ being the dimensionless slip length; $D=1/Pe_s$ is the inverse of the surface Péclet number to reflect the strength of surface diffusion of surfactant.

With a soluble surfactant, the effects would be similar to those produced by an insoluble surfactant having a large surface diffusion coefficient since the interfacial surfactant concentration gradient would probably be diminished by surfactant adsorption/desorption from/to the bulk. Hence, much like figure 4, it is likely that the resulting film thickness might display three distinct regimes as Ca is varied due to the competition between surfactant-induced film thickening and slip-induced film thinning.

In practice, because wall slip can be rendered by using polymer liquids and also because the solubility of a surfactant can be adjusted by its added amount, it is possible to test our findings by selecting a proper surfactant–polymer–liquid system, as discussed in § 4. If this can be done and our predictions can be confirmed by experiments, one might be able to make use of wall slip and surfactant together to have a more precise control of the deposited film thickness for Landau–Levich–Bretherton flow. One can also employ such a flow to quantify the amount of wall slip by having a more accurate determination of the slip length.

Acknowledgement

Y.-C. Li and H.-H. Wei acknowledge support by the Ministry of Science and Technology of Taiwan.

Appendix A

This appendix provides additional details about the method we employed for determining the film thickness by solving (2.12*a*) numerically. First, we define new variables:

$$\eta=\frac{H}{B},\quad \xi=\frac{X}{B}. \tag{A 1a,b}$$

Then, (2.12*a*) is reduced to

$$\eta_{\xi\xi\xi}=\frac{3(\eta-1)}{S\eta^{3}}, \tag{A 2}$$

where

$$S=1+3\frac{\overline{\overline{\Lambda}}}{\eta}-\frac{3}{4}\frac{\overline{M}\eta(1+2\overline{\overline{\Lambda}}/\eta)^{2}}{\overline{M}\eta(1+\overline{\overline{\Lambda}}/\eta)+\overline{D}}, \tag{A 3}$$

with $\overline{\overline{A}} = \overline{A}/B$ and $\overline{M} = M/B$. As we approach the uniform film region, $\xi \to -\infty$, an asymptotic solution to (A 2) can be obtained by linearizing (A 2) about $\eta = 1$, and is given by

$$\eta \to 1 + A\mathrm{e}^{(3/S_\infty)^{1/3}\xi} \quad \text{as } \xi \to -\infty, \tag{A 4}$$

where A is an integration constant and $S_\infty = S|_{\eta=1}$. In the neighbourhood of the bubble tip, $\xi \to \infty$, the asymptotic solution to (A 2) must have constant curvature (since $\eta_{\xi\xi\xi} \to 0$), and can be expressed as

$$\eta = \tfrac{1}{2}P(\eta - \eta_0)^2 + Q, \tag{A 5}$$

where $P = \lim_{\xi\to\infty} \eta_{\xi\xi}$, Q and η_0 are constants which are determined numerically. The dimensional form of (A 5) is

$$h = \frac{1}{2}PCa^{2/3}\frac{(x - x_0)^2}{b} + Qb. \tag{A 6}$$

Thus, the radius of curvature at the tip is $b/PCa^{2/3}$, and to leading order (for $Ca \ll 1$) this must equal to the tube radius R. Therefore,

$$B = \frac{b}{RCa^{2/3}} = P. \tag{A 7}$$

That is, the scaled thickness parameter B is equal to the integration constant P. In order to determine P, (A 2) is first rewritten as a system of three first-order differential equations and then solved numerically using the initial value problem package LSODE (Hindmarsh 1983). The initial conditions come from the asymptotic solution derived above, and because the system is translational invariant, they can be defined at $\xi = 0$:

$$\eta(0) = 1 + A, \quad \eta_\xi(0) = A(3/S_\infty)^{1/3}, \quad \eta_{\xi\xi}(0) = A(3/S_\infty)^{2/3}. \tag{A 8a–c}$$

In the calculations presented in this paper, $A = 10^{-8}$, and the size of the domain is chosen to be large enough so that $\eta_{\xi\xi}(\xi = \xi_{max})$ is approximately constant. It should be noted that for given $\overline{\overline{A}}$, $\overline{M}$ and $\overline{D}$, the system of differential equations is solved just once in order to determine P and hence B.

REFERENCES

BRETHERTON, F. P. 1961 The motion of long bubbles in tubes. *J. Fluid Mech.* **10** (2), 166–188.

CAMPANELLA, O. H. & CERRO, R. L. 1984 Viscous flow on the outside of a horizontal rotating cylinder: the roll coating regime with a single fluid. *Chem. Engng Sci.* **39** (10), 1443–1449.

CHOI, C.-H. & KIM, C.-J. 2006 Large slip of aqueous liquid flow over a nanoengineered superhydrophobic surface. *Phys. Rev. Lett.* **96** (6), 066001.

DELACOTTE, J., MONTEL, L., RESTAGNO, F., SCHEID, B., DOLLET, B., STONE, H. A., LANGEVIN, D. & RIO, E. 2012 Plate coating: influence of concentrated surfactants on the film thickness. *Langmuir* **28** (8), 3821–3830.

DE GENNES, P. G. 1985 Wetting: statics and dynamics. *Rev. Mod. Phys.* **57** (3), 827–863.

HINDMARSH, A. C. 1983 ODEPACK, a systematized collection of ODE solvers. In *Scientific Computing* (ed. R. S. Stepleman, M. Carver, R. Peskin, W. F. Ames & R. Vichnevetsky), IMACS Transactions on Scientific Computation, vol. 1, pp. 55–64. North-Holland.

KALLIADASIS, S. & CHANG, H.-C. 1994 Apparent dynamic contact angle of an advancing gas–liquid meniscus. *Phys. Fluids* **6** (1), 12–23.

KRECHETNIKOV, R. & HOMSY, G. M. 2006 Surfactant effects in the Landau–Levich problem. *J. Fluid Mech.* **559**, 429–450.

LANDAU, L. & LEVICH, B. 1942 Dragging of a liquid by a moving plate. *Acta Physicochim. USSR* **17**, 42–54.

LI, Y.-C., LIAO, Y.-C., WEN, T.-C. & WEI, H.-H. 2014 Breakdown of the Bretherton law due to wall slippage. *J. Fluid Mech.* **741**, 200–227.

LIAO, Y.-C., LI, Y.-C., CHANG, Y.-C., HUANG, C.-Y. & WEI, H.-H. 2014 Speeding up thermocapillary migration of a confined bubble by wall slip. *J. Fluid Mech.* **746**, 31–52.

LIAO, Y.-C., LI, Y.-C. & WEI, H.-H. 2013 Drastic changes in interfacial hydrodynamics due to wall slippage: slip-intensified film thinning, drop spreading, and capillary instability. *Phys. Rev. Lett.* **111**, 136001.

MATTHEWS, M. T. & HILL, J. M. 2009 On three simple experiments to determine slip lengths. *Microfluid. Nanofluid.* **6** (5), 611–619.

PARK, C. W. 1991 Effects of insoluble surfactants on dip coating. *J. Colloid Interface Sci.* **146** (2), 382–394.

PIROIRD, K., CLANET, C. & QUÉRÉ, D. 2011 Detergency in a tube. *Soft Matt.* **7** (16), 7498–7503.

QUÉRÉ, D. 1999 Fluid coating on a fiber. *Annu. Rev. Fluid Mech.* **31**, 347–384.

RAMDANE, O. O. & QUÉRÉ, D. 1997 Thickening factor in Marangoni coating. *Langmuir* **13** (11), 2911–2916.

RATULOWSKI, J. & CHANG, H.-C. 1990 Marangoni effects of trace impurities on the motion of long gas-bubbles in capillaries. *J. Fluid Mech.* **210**, 303–328.

SCHWARTZ, L. W., PRINCEN, H. M. & KISS, A. D. 1986 On the motion of bubbles in capillary tubes. *J. Fluid Mech.* **172**, 259–275.

SHEN, A. Q., GLEASON, B., MCKINLEY, G. H. & STONE, H. A. 2002 Fiber coating with surfactant solutions. *Phys. Fluids* **14** (11), 4055–4068.

STONE, H. A. 1990 A simple derivation of the time-dependent convective-diffusion equation for surfactant transport. *Phys. Fluids* A **2** (1), 111–112.

STONE, H. A. 2010 Interfaces: in fluid mechanics and across disciplines. *J. Fluid Mech.* **645**, 1–25.

WILSON, S. D. R. 1982 The drag-out problem in film coating theory. *J. Engng Maths* **16** (3), 209–221.